

2017

Electrosensitization Increases Antitumor Effectiveness of Nanosecond Pulsed Electric Fields In Vivo

Claudia Muratori

Old Dominion University, cmurator@odu.edu

Andrei G. Pakhomov

Old Dominion University, apakhomo@odu.edu

Loree Heller

Old Dominion University, lheller@odu.edu

Maura Casciola

Old Dominion University

Elena Gianulis

Old Dominion University

See next page for additional authors

Follow this and additional works at: https://digitalcommons.odu.edu/bioelectrics_pubs



Part of the [Biomedical Engineering and Bioengineering Commons](#), [Medical Sciences Commons](#), and the [Oncology Commons](#)

Repository Citation

Muratori, Claudia; Pakhomov, Andrei G.; Heller, Loree; Casciola, Maura; Gianulis, Elena; Grigoryev, Sergey; Xiao, Shu; and Pakhomova, Olga N., "Electrosensitization Increases Antitumor Effectiveness of Nanosecond Pulsed Electric Fields In Vivo" (2017). *Bioelectrics Publications*. 142.

https://digitalcommons.odu.edu/bioelectrics_pubs/142

Original Publication Citation

Muratori, C., Pakhomov, A. G., Heller, L., Casciola, M., Gianulis, E., Grigoryev, S., . . . Pakhomova, O. N. (2017). Electrosensitization increases antitumor effectiveness of nanosecond pulsed electric fields in vivo. *Technology in Cancer Research and Treatment*, 16(6), 987-996. doi:10.1177/1533034617712397

Authors

Claudia Muratori, Andrei G. Pakhomov, Loree Heller, Maura Casciola, Elena Gianulis, Sergey Grigoryev, Shu Xiao, and Olga N. Pakhomova

Electrosensitization Increases Antitumor Effectiveness of Nanosecond Pulsed Electric Fields *In Vivo*

Technology in Cancer Research & Treatment
2017, Vol. 16(6) 987–996
© The Author(s) 2017
Reprints and permission:
sagepub.com/journalsPermissions.nav
DOI: 10.1177/1533034617712397
journals.sagepub.com/home/tct


Claudia Muratori, PhD¹, Andrei G. Pakhomov, PhD¹, Loree Heller, PhD¹, Maura Casciola, PhD¹, Elena Gianulis, PhD¹, Sergey Grigoryev, PhD¹, Shu Xiao, PhD¹, and O. N. Pakhomova, PhD¹

Abstract

Nanosecond pulsed electric fields are emerging as a new modality for tissue and tumor ablation. We previously reported that cells exposed to pulsed electric fields develop hypersensitivity to subsequent pulsed electric field applications. This phenomenon, named electrosensitization, is evoked by splitting the pulsed electric field treatment in fractions (split-dose treatments) and causes *in vitro* a 2- to 3-fold increase in cytotoxicity. The aim of this study was to show the benefit of split-dose treatments for *in vivo* tumor ablation by nanosecond pulsed electric field. KLN 205 squamous carcinoma cells were embedded in an agarose gel or grown subcutaneously as tumors in mice. Nanosecond pulsed electric field ablations were produced using a 2-needle probe with a 6.5-mm interelectrode distance. In agarose gel, splitting a pulsed electric field dose of 300, 300-ns pulses (20 Hz, 4.4–6.4 kV) in 2 equal fractions increased cell death up to 3-fold compared to single-train treatments. We then compared the antitumor effectiveness of these treatments *in vivo*. At 24 hours after treatment, sensitizing tumors by a split-dose pulsed electric field exposure (150 + 150, 300-ns pulses, 20 Hz, 6.4 kV) caused a 4- and 2-fold tumor volume reduction as compared to sham and single-train treatments, respectively. Tumor volume reduction that exceeds 75% was 43% for split-dose-treated animals compared to only 12% for single-dose treatments. The difference between the 2 experimental groups remained statistically significant for at least 1 week after the treatment. The results show that electrosensitization occurs *in vivo* and can be exploited to assist *in vivo* cancer ablation.

Keywords

nanosecond pulsed electric fields (nsPEF), irreversible electroporation, tumor ablation, nanoporation, electrosensitization

Abbreviations

DT, doubling time; EMEM, Eagle's minimum essential medium; IRE, irreversible electroporation; nsPEF, nanosecond pulsed electric fields; PBS, phosphate-buffered saline; PEF, pulsed electric fields; PI, propidium iodide; Pr, propidium; PRR, pulse repetition rate; ROI, region of interest; ROS, reactive oxygen species

Received: February 15, 2017; Revised: April 24, 2017; Accepted: May 04, 2017.

Introduction

Several local ablative therapies have been explored as innovative treatments to fight cancer. The advantages of these procedures include increased safety, less scarring, fast recovery, and decreased length of hospital stay.¹ Irreversible electroporation (IRE) is a promising new minimally invasive technique for tumor ablation. Irreversible electroporation uses high-intensity pulsed electric fields (PEF) of 100 μ s duration to cause irreparable cell damage and destroy tissues.² Compared to other conventional ablation methods, such as radiofrequency heating and cryoablation, IRE treatments preserve vital

structures and major blood vessels within the ablated zone.³ Irreversible electroporation was found particularly efficient at treating tumors less than 3.0 cm.² However, larger lesions

¹ Frank Reidy Research Center for Bioelectrics, Old Dominion University, Norfolk, VA, USA

Corresponding Author:

Claudia Muratori, PhD, Old Dominion University, 4211 Monarch Way, Norfolk, VA 23508, USA.
Email: cmurator@odu.edu



require the repositioning of the electrodes, making the procedure more complex. Because of this limitation, ongoing research focuses on establishing well-defined treatment planning protocols and improving the treatment delivery methods.⁴⁻⁶

Recently, IRE protocols have been extended to nanosecond pulse durations. Nanosecond pulsed electric fields (nsPEF) have been shown to cause complete regression of murine melanoma with no recurrence.⁷⁻⁹ Nanosecond pulsed electric field induced apoptosis in tumor cells and disrupted tumor's blood supply.⁸ Nanosecond pulsed electric field effects encompass nanoporation of membranes (plasma membrane, endoplasmic reticulum, and mitochondria),¹⁰⁻¹⁵ Ca^{2+} uptake from the outside and release from the endoplasmic reticulum,^{13,14,16,17} destruction of the cytoskeleton and cell blebbing,¹⁸⁻²¹ activation of signaling pathways,²²⁻²⁴ and induction of necrosis and apoptosis.^{10,25-27} The diversity of these effects is promising for future therapeutic applications of nsPEF.

We previously reported a gradual intensification in the sensitivity of electroporated cells to incoming PEF treatments, a phenomenon that has been named electrosensitization.²⁸ Since electrosensitization develops with time, this phenomenon can be engaged by either using a single dose of pulses delivered at a low pulse repetition rate (PRR) or splitting a high PRR dose into fractions separated by a proper latency time. Indeed, the PRR is one of the key factors that determine the efficiency of electroporation, and many studies have reported the higher efficiency of low PRR.²⁸⁻³⁴ Our standard electrosensitization protocol consists in delivering 2 high-frequency trains of pulses separated by a proper interval.^{28,35-37} Engaging electrosensitization increases the cytotoxic effect of a PEF treatment 2- to 3-fold and causes a significant reduction in the PEF lethal dose.

Electrosensitization has also been shown to improve the electroporative uptake of the cytostatic agent bleomycin.³⁵ Bleomycin is used in combination with PEF in electrochemotherapy protocols.³⁸⁻⁴⁰ Electrosensitization profoundly increased the electroporation-assisted bleomycin uptake and caused an increase in lethality comparable to a 10-fold increase in bleomycin concentration when using a single PEF dose.³⁵

Recently, the increase in the ablation zone created by split-dose protocols engaging electrosensitization has been visualized in 3-dimensional (3D) cultures. In agarose-embedded KLN 205 cells and matrigel spheroids, dose fractionation increased the ablation volume and cell death up to 2- to 3-fold compared to single-train treatments.³⁷

To date, electrosensitization phenomenon has been reported *in vitro* for PEF durations ranging from 60 ns to 100 μs and pulse amplitudes from 1.8 to 13.3 kV/cm, in multiple cell lines (CHO, B16, U937, Jurkat, and KLN 205), and for diverse experimental settings (cells in suspension, substrate-attached cells, cells embedded in agarose gel, or grown as spheroids in matrigel).^{28,35-37}

In this study, we compared the *in vivo* antitumor efficacy of split- and single-dose nsPEF treatments. Engaging electrosensitization caused increased tumor reduction showing its benefit for tumor ablation *in vivo*.

Electrosensitization can potentially enable the use of lower electric field amplitudes to achieve the same or better ablation effect than standard single-train protocols. Attaining the therapeutic effect at much lower exposure doses translates into a reduction in the thermal damage due to the Joule heating and could potentially minimize IRE known side effects such as pain, muscle contraction, and cardiac arrhythmias when treatments are done in the proximity of the heart.

Materials and Methods

Cell Line and Media

Experiments were performed using a mouse squamous cell carcinoma KLN 205 cell line (ATCC, Manassas, Virginia).⁴¹ Cells were cultured in Eagle's minimum essential medium with L-glutamine (ATCC), supplemented with 10% (v/v) fetal bovine serum (Atlanta Biologicals, Norcross, Georgia), 100 U/mL penicillin and 0.1 mg/mL streptomycin (Mediatech Cellgro, Herdon, Virginia).

Pulsed Electric Field Exposure

The same PEF exposure system was used for both 3D cultures and tumors in mice.

Trapezoidal pulses of 300 ns duration were produced by a custom pulse generation system with an output impedance of 100 Ω , adjustable pulse amplitude (up to 15 kV), duration (150-2000 ns), and frequency (1-100 Hz; Tangers Electronics, Norfolk, Virginia; Figure 1A). Pulsed electric field was delivered by a PEF-delivering 2-needle electrode probe made from 0.5 mm diameter hollow syringe needles. The edge-to-edge distance between the needles was 6.5 mm with a maximum penetration capacity in agarose culture or the mouse skin of 5 mm (Figure 1B). To produce pulse trains of predetermined duration at selected repetition rates, the generator was triggered externally from a model S8800 stimulator (Grass Instrument Co, Quincy, Massachusetts). Pulse amplitude was monitored in all experiments, using a 200 MHz, 1 GS/s DSO5202B digital oscilloscope (Antek, Qingdao City, China). The shape of the electric pulse at 6.4 kV is reported in Figure 1C.

Pulsed electric field delivery to cells embedded in agarose gel was accomplished by mounting the electrodes on a micro-manipulator to enable accurate and steady positioning of the needles within the gel with cells in a 35-mm Petri dish. For accurate comparison, different PEF treatments and sham exposure (no pulses delivered) were performed in the same cell sample for a maximum of 6 exposures per dish. We previously reported that electrosensitization develops only if the electric field is above the threshold for electroporation.⁴² In our experiments, each exposure was spaced 1 cm from the previous one to avoid any "electroporation-preconditioning" of the area. In fact, for 300 ns pulses applied at 6.4 kV (which is the highest electric field used in the *in vitro* experiments shown in Figure 4), the electric field at 1 cm from the electrodes is 0.8 kV/cm. Based on the electroporation thresholds found, for

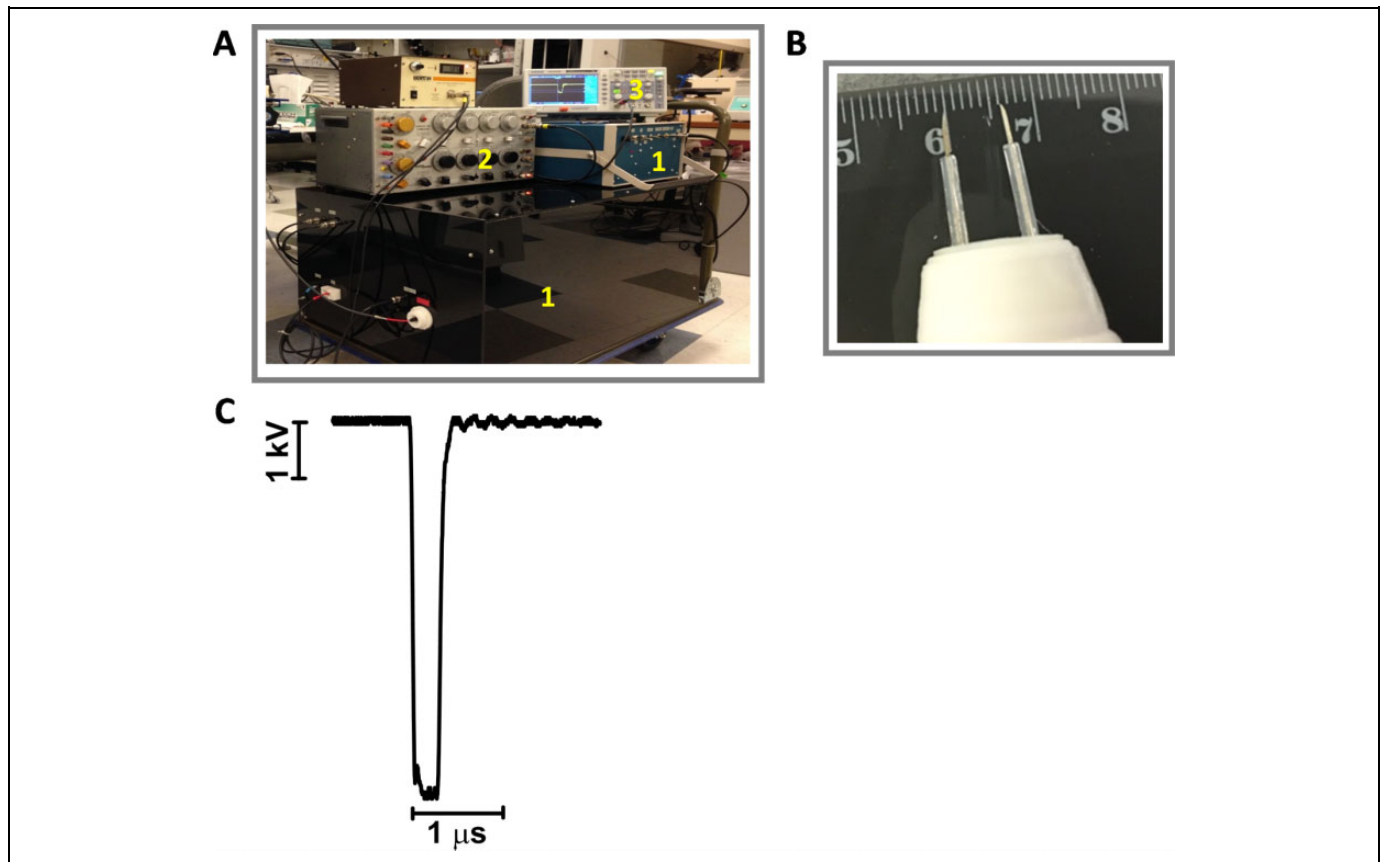


Figure 1. Pulsed electric field (PEF) exposure system. A, The pulse generator (1) was triggered externally from a stimulator (2), and the pulse amplitude and shape were monitored using a digital oscilloscope (3). B, The 2-needle probe showing the 6.5 mm separation. C, The shape of the electric pulse at 6.4 kV.

200 and 600 ns pulses, which are 1.5 to 1.9 and 1 kV/cm, respectively,^{43,44} 0.8 kV/cm gives a good safety margin being about 2-fold below the expected threshold for 300 ns pulses.

For tumor PEF treatments, mice were anesthetized by inhalation of 3% isoflurane in air (Patterson Veterinary, Devens, Massachusetts). The 2-needle electrode was inserted at the opposite margins of the tumor by lifting the overlying skin. Ultrasound conductive gel (Parker Laboratories, Fairfield, New Jersey) was used to ensure an efficient electrical continuity. During PEF treatments, the probe was held by hand and readjusted to the proper position between trains if needed. Animals in the sham control group underwent anesthesia and the probe insertion procedure but no PEF delivery. Tumors were subjected to a single-PEF treatment with 1 electrode insertion.

Electric Field Simulation and Temperature Measurements

To quantify the electric field distribution, we carried out a 3D numerical simulations using the commercial finite element method solver COMSOL Multiphysics, Release 5.0. Figure 2A shows the electric field at the cell location between the electrodes, 3.8 mm above the plane of the Petri dish. The dish was modeled as a 2-mm thick layer of polystyrene. To match the experimental

conditions, the electrodes (modeled as stainless steel) were positioned perpendicular to the Petri dish, 1 mm above it. The electric currents interface was used to solve Maxwell equations under the assumption of steady-state conditions, for which:

$$\nabla \cdot (-\sigma \nabla V) = 0 \quad (1)$$

This equation is solved for the voltage field, V , which is used to compute the electric field, $E = -\nabla V$, and the current, $J = \sigma E$, where σ is the material conductivity.

Since, the calculations were based on an electrostatic model that disregards the dispersive properties of the medium: this was possible since the dielectric relaxation time for a buffer conductivity of 1.4 S/m would be on the order of few nanoseconds, much shorter than the nsPEF duration considered.⁴⁵⁻⁴⁷ The tetrahedral mesh chosen to discretize the domain of simulation (sphere of air with radius of 21.8 mm) resulted in a total of 668 169 elements, with a minimum size of 0.065 mm and a maximum size of 1.530 mm. Quadratic elements were used throughout the solution domain, giving 0.9×10^6 degrees of freedom. Under these conditions, the mean electric field and its standard deviation (SD) in the region of interest (ROI), defined as a 1 mm \times 1 mm square between the electrodes, was 0.082 (0.001) kV/cm for 100 V of input. The coefficient of variation in percent, namely the ratio of

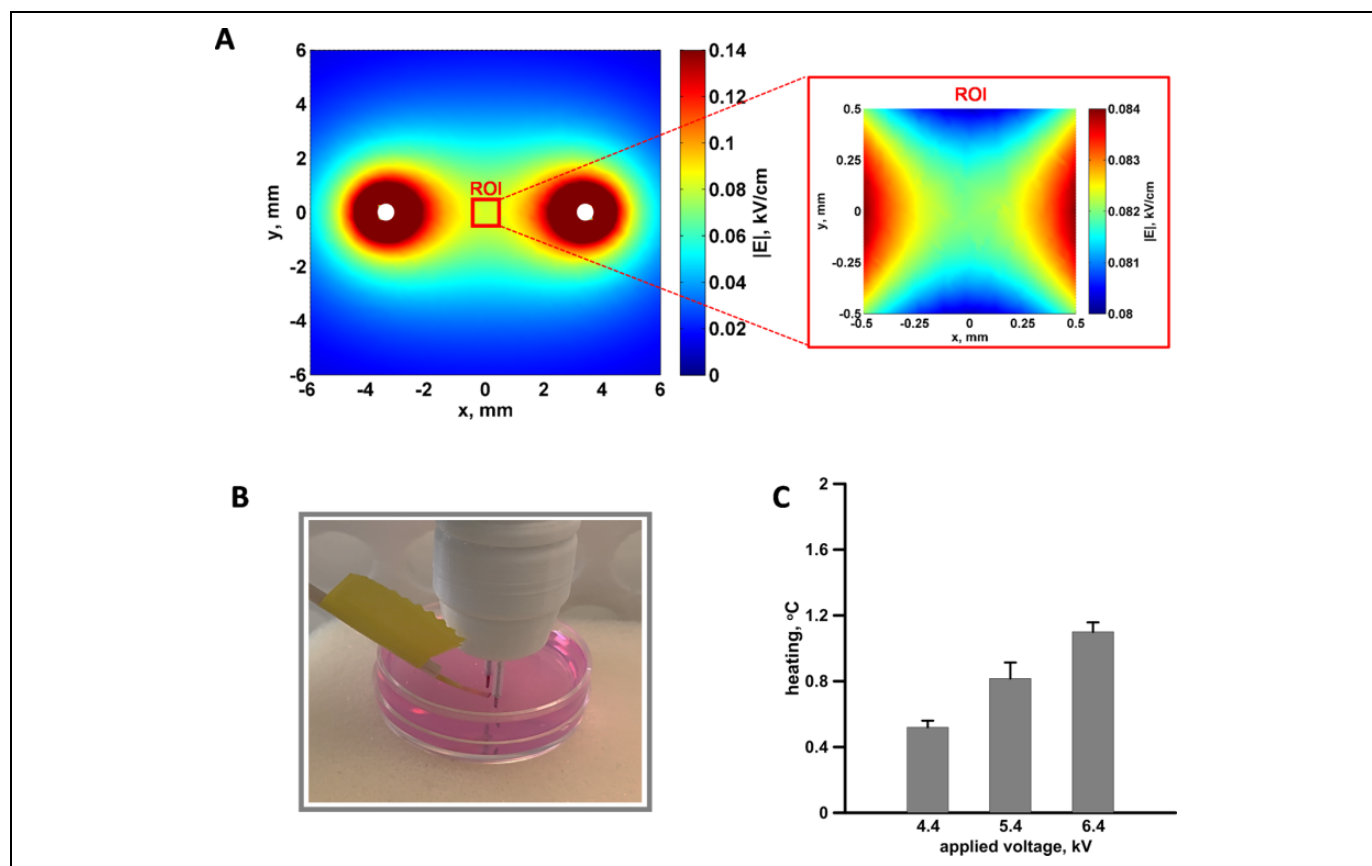


Figure 2. The electric field distribution (A) and temperature measurements (B and C) in 3-dimensional (3D) cell cultures. The electric field distribution in the plane perpendicular to the needle electrodes (white circles) and 3.8 mm above the bottom of the Petri dish (left) and within the 1 mm² region of interest (ROI) used for the quantification of the propidium (Pr) fluorescence (right). Note that the 2 maps have different color scales. For 100 V applied between the electrodes, the mean electric field in the ROI was 0.082 kV/cm with 1.2% variation. B, The fiber optic probe, used to measure the temperature, placed in the center of the gap between the electrodes. C, Temperature rise measured after 300, 300 ns pulses (20 Hz) delivered at the indicated voltages.

the SD over the mean value of the electric field, was 1.2% showing the high homogeneity of the electric field in the ROI.

In the 3D cultures, the local heating was measured using a fiber optic ReFlex-4 thermometer (Nortech Fibronic, Quebec City, Canada). The fiber optic probe was inserted into the agarose culture in the center of the gap between the electrodes (Figure 2B). By the end of PEF exposure, the measured values for 300, 300-ns pulses at 4.4, 5.4, and 6.4 kV delivered at 20 Hz averaged 0.5, 0.8, and 1.1°C, respectively (Figure 2C). In practice, PEF trains that were used to study electrosensitization effects (up to 300 pulses) did not raise the temperature to potentially damaging levels.

Cell Culture and PEF Cytotoxicity in 3D Cultures

Three-dimensional cultures in agarose were described in detail previously.³⁷ Briefly, the bottom of a 35-mm dish was coated with 3 mL of 2.5% low-gelling-temperature agarose (Sigma-Aldrich, St Louis, Missouri) in the growth medium. Cells were resuspended at 5×10^6 cell/mL in 1% agarose in the growth medium, and 1.5 mL of this suspension was pored over the presolidified 2.5% agarose base layer. The samples were incubated at 4°C for 5 minutes to speed up agarose jellification thus

avoiding cell sedimentation, covered with 0.5 mL of media, and kept in the incubator for 30 minutes before PEF treatment.

The agarose cultures were analyzed 2 hours after exposure. Dead cells were stained using 4 µg/mL of propidium iodide (PI; Sigma-Aldrich) in phosphate-buffered saline (PBS). Thirty minutes before the analysis, the growth medium was replaced with 1 mL of PI solution. Images of the ablation zone were acquired using an Olympus SZX16 fluorescence stereo microscope (Olympus America, Hamden, Connecticut) equipped with a Hamamatsu C9100 EM-CCD camera using a 0.9×, 0.44 NA objective.

Images were analyzed with MetaMorph version 7.5.2 software (Molecular Devices, Foster City, California). Propidium (Pr) signal was quantified in the center of the gap between the electrodes within a region of 1 mm² with almost uniform electric field (Figure 2A). For each image, the fluorescence intensity of the exposed area was corrected for the background fluorescence.

Murine Tumor Model

Seven- to 8-week-old DBA/2 J female mice (Jackson Laboratory, Bar Harbor, Maine) were anesthetized by inhalation of 3% isoflurane and inoculated subcutaneously in the left dorsolateral

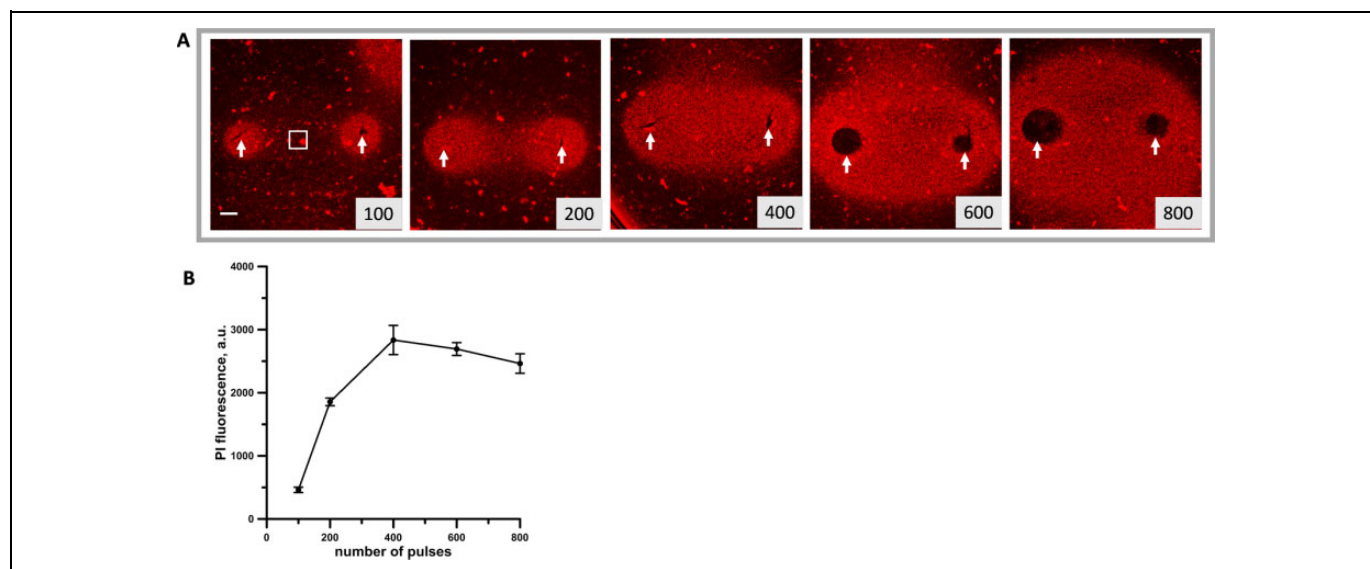


Figure 3. Analysis of the cytotoxic effect of 300 ns, 6.4 kV pulses in KLN 205 cells embedded in agarose. A, The ablation area between and around the 6.5-mm gap pulsed electric field (PEF)-delivering electrodes (arrows) was visualized by propidium (Pr) uptake by dead cells. Images were taken 2 hours after exposure to the indicated number of pulses. Scale bar: 1 mm. B, Quantification of the cytotoxic effect by the mean intensity of Pr fluorescence (as measured within the region of interest shown in (A)). Mean \pm standard error (SE), $n = 3$. Note signal saturation at 400 to 800 pulses, which indicates killing of 100% of cells within the studied region.

flank region with 1×10^6 KLN 205 cells in 50 μ L of PBS. Mice were housed in individually ventilated cages in groups of 5 under pathogen-free conditions. Tumors were allowed to grow to a volume of approximately 35 to 45 mm^3 before PEF treatment. Tumor growth was measured at 24 hours posttreatment and twice weekly using a digital caliper, and volumes (v) were calculated using a standard formula $v = ab^2\pi/6$, where a is the longest diameter, and b is the next longest diameter perpendicular to a . Mice were humanely euthanized when the tumor reached 800 mm^3 . Tumors were considered eliminated when no recurrence was detected within 100 days after treatment. Tumor doubling time (DT) was calculated using the Schwartz formula.⁴⁸

This experiment protocol was approved by the Old Dominion University Institutional Animal Care and Use Committee (permit number: 15-009).

Statistical Analysis

Data are presented as mean \pm standard error for n independent experiments. Statistical analyses were performed using a 2-tailed t test where $P < .05$ was considered statistically significant. Statistical calculations, including data fits, and data plotting were accomplished using Grapher 11 (Golden Software, Golden, Colorado).

Results

Quantification of the Electrosensitization Phenomenon In Vitro in 3D Agarose Cultures

In our previous publications, the electrosensitization phenomenon has been investigated by using exposure system with 1 mm

distance between the PEF-delivering electrodes (ie, 1-mm gap cuvettes or a 1-mm gap 2-needle probe).^{28,35,37} However, because our *in vivo* model envisages the treatment of tumors of about 5 mm in diameter, here, we studied the effect of dose fractionation on the size of ablation zone generated in a 3D agarose culture by applying a voltage across a 6.5-mm gap.

As a first step, we established the PEF conditions needed to kill in 2 hours 100% of cells between the PEF-delivering electrodes. For consistency with our previous research,³⁷ we used pulses of 300 ns duration. The effect of increasing number of pulses 300 ns (6.4 V, 20 Hz) on KLN 205 cells embedded in 1% agarose was visualized by the Pr fluorescence in the lethally damaged cells. Figure 3 shows that significant cell killing started after 200 or more pulses. To quantify this effect, we measured the Pr fluorescence intensity in a region of 1 mm^2 in the center of the gap between the electrodes where cells experienced nearly uniform electric field (Figures 3A and 4). Propidium fluorescence intensity reached a plateau at 400 to 800 pulses indicating that at these doses, 100% of the cells in the quantified area were killed. Therefore, in the subsequent experiments, a parallel control exposure of 600 pulses was used as a reference point for Pr fluorescence that corresponds to 100% cell death.

To investigate the electrosensitization phenomenon, 300 pulses (300 ns, 20 Hz) were delivered either as a single train or as 2 trains with a 2-minute interval (also referred to as single- and split-dose treatments below), and the voltage applied was varied from 4.4 to 6.4 kV. Figure 4A shows for a representative experiment that fractionated treatments produced larger Pr-positive region. Maximum sensitization effect was seen at 4.4 kV (3.6 kV/cm in the center between the electrodes) where

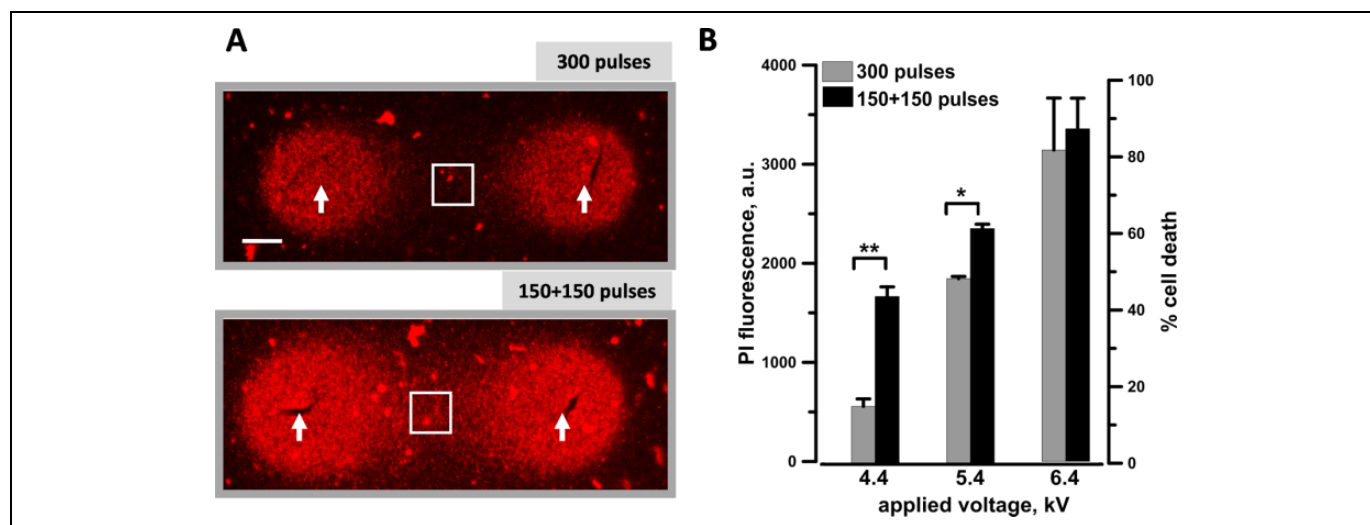


Figure 4. Electrosensitization efficiency at different applied voltages when using a pulsed electric field (PEF)–delivering probe with 6.5 mm gap between the electrodes. KLN 205 cells seeded in 1% agarose were exposed to either a single train of 300 pulses (300 ns, 20 Hz) or 2 trains of 150 pulses each with a 2-minute interval. The pulse amplitude was varied from 4.4 to 6.4 kV. A, Each sample at 4.4 kV, a representative propidium (Pr) fluorescence image. The arrows identify the nanosecond pulsed electric field (nsPEF) delivering electrodes. Scale bar: 1 mm. The quantification in (B) shows the Pr uptake (left Y-axis) and the percentage of cell death (right Y-axis) measured within the region of interest (white square) shown in (A). Mean \pm standard error (SE), $n = 5$ to 6. * $P < .01$ and ** $P < .001$.

the Pr signal increased 3 times and lethality increased from 12%-16% to 41%-46% (Figure 4B). At the next higher amplitude (5.4 kV), fractionated doses were significantly more efficient as well. However, at 6.4 kV where the single dose already killed 80% of the cells, approaching the fluorescence saturation point, splitting the PEF train in fractions had no additional effect.

Overall, in these *in vitro* experiments, we established the conditions necessary to achieve efficient sensitization effect using a large gap PEF-delivering probe.

Electrosensitization Assists Tumor Ablation by nsPEF *In Vivo*

The lethal electric field threshold for cells in medium may considerably differ from that of tumors *in vivo*.^{49,50} Hence, the PEF conditions to see electrosensitization *in vivo* needed to be tested in preliminary experiments. Our *in vitro* data showed that splitting in fractions a PEF dose that kills 20% to 50% of the cells, causes maximum electrosensitization effect. To identify the PEF dose that matches these conditions *in vivo*, we investigated the antitumor efficacy of 300 ns pulses over a range of electric field amplitudes. At 24-hour posttreatment, 300, 300-ns pulses (20 Hz) at 6.4 kV caused 50% tumor reduction, and therefore this PEF dose was selected to study the electrosensitization phenomenon *in vivo* (data not shown).

At the time of treatment, tumors were on average 40.2, 41.2, and 39.2 mm³ for sham exposure, single-dose, and split-dose groups, respectively (Table 1). Tumor size was assessed 24 hours after the treatment and then monitored twice weekly for 3 weeks. At 24 hours after the treatment, split-dose protocols

Table 1. Average Tumor Size on the Day of PEF Treatment and the Number of Animals in the Experimental Groups.

| Groups | Sham | 300 Pulses | 150 + 150 Pulses |
|--|----------------|--------------|------------------|
| Average tumor size at the time of treatment, mm ³ | 40.2 \pm 3.7 | 41.2 \pm 3 | 39.2 \pm 2.6 |
| Number of animals per group | 15 | 17 | 14 |

Abbreviation: PEF, pulsed electric field.

(150 + 150 pulses) with intertrain interval of 2 minutes, caused a 4- and 2-fold tumor volume reduction as compared to sham and single-dose exposure controls, respectively (Figure 5A). In the split-dose group, 43% of the animals exceeded the 75% level of tumor volume reduction, whereas only 12% of single-dose treated animals achieved a similar ablation level (Figure 5B). The difference between single- and split-dose treatments remained statistically significant for at least 1 week after the treatment (Figure 5A). No differences in tumor DT were observed between the different experimental groups suggesting that the tested nsPEF did not trigger any tumor growth inhibition besides their lethal effect at the time of treatment (Figure 5C). Finally, none of the animals were cured with the single-dose protocol, whereas 1 split-dose treatment resulted in complete tumor regression with no recurrence (tumor-free animal for 100 days).

Discussion

In this study, we show, for the first time, that split-dose nsPEF treatments engaging electrosensitization facilitate tumor

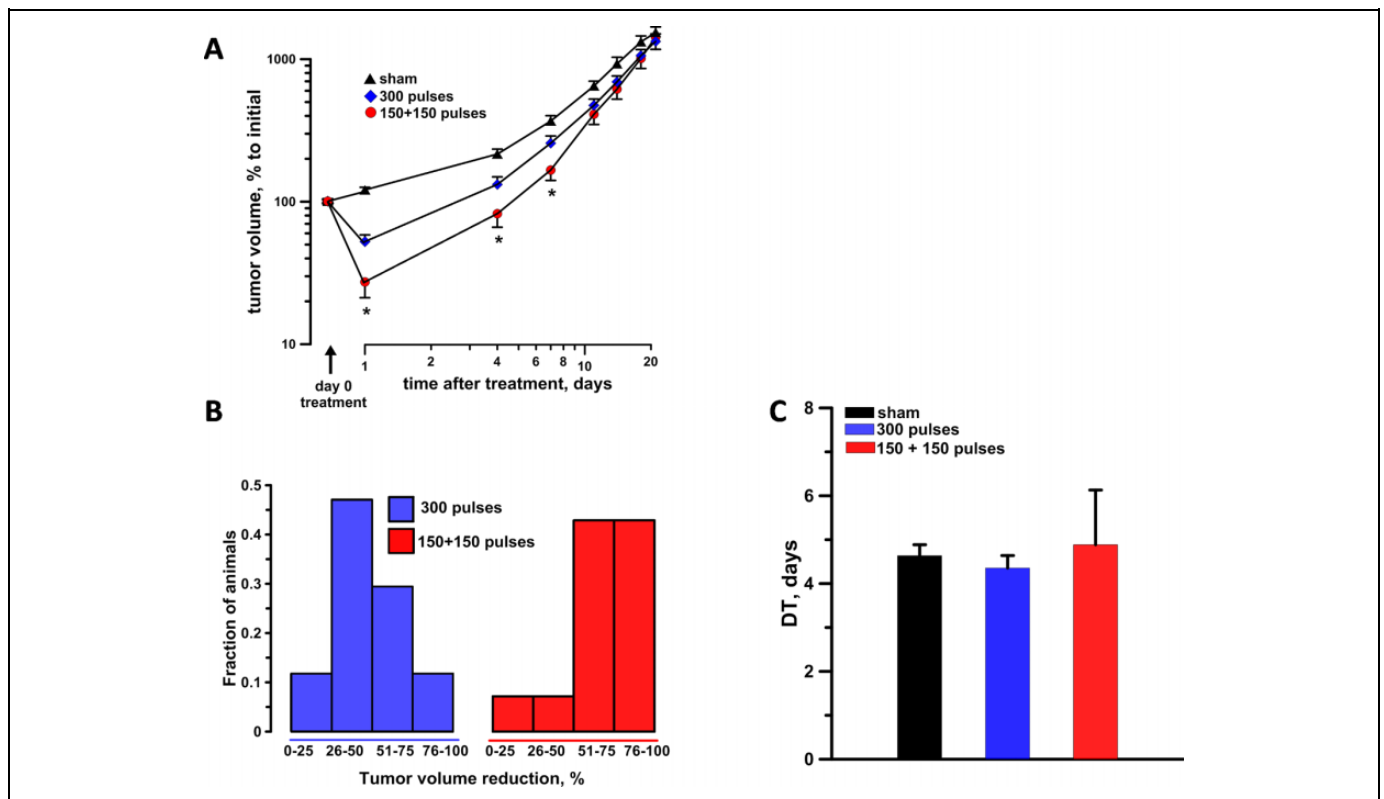


Figure 5. *In vivo* split-dose treatments engaging electrosensitization increase the antitumor effectiveness of nsPEF. A, Tumor growth curves in sham exposure, single-dose 300 pulses (300 ns, 6.4 kV, 20 Hz), and split-dose 150 + 150 pulses with 2-minute interval experimental groups. For each animal, the data were normalized to the tumor volume measured immediately before treatment. B, The tumor reduction frequency histogram at 24 hours after the treatment. C, The tumor doubling time. Mean \pm standard error (SE), $n = 15, 17,$ and 14 for sham, split- and single-dose groups, respectively. * $P < .05$ for the difference between single- and split-dose groups.

destruction *in vivo* as well as *in vitro*. Despite delivering equivalent doses, splitting a PEF train in 2 fractions with a 2-minute interval caused a 2-fold tumor volume reduction compared to single-train treatments. All mice treated with the split-dose treatment experienced a significant reduction in tumor volume, and this difference remained statistically significant for a week. However, with the PEF dose used in the study (300, 300-ns pulses, 20 Hz at 6.4 kV), engaging electrosensitization did not cause persistent tumor regression. Maximum electrosensitization effect may develop within a certain range of pulse amplitudes, durations, frequencies, number of pulses, and trains. It remains to be fully established how various PEF parameters affect the development of electrosensitization. In this study, because the needles penetrated the body of the mouse, the range of PEF doses that could be tested was limited by the risk of harming internal organs. For instance, 6.4 kV was the highest PEF amplitude that was also well tolerated by the animals. We therefore believe that the results of this pilot study can be further improved by a careful design of the PEF-delivering electrodes thus allowing to optimize the PEF parameters *in vivo*.

We previously reported that the time interval between trains affects cell killing by electrosensitization. In KLN 205 embedded in 3D agarose, dose fractionation enhanced Pr uptake when the intertrain interval reached 100 seconds.³⁷

However, the time course of electrosensitization *in vitro* and *in vivo* in tumors may differ. In this study, we used 2-minute intervals that might have not been optimal to cause maximum facilitation of cell killing by engaging electrosensitization. Future work will focus on the optimization of the intertrain interval to fully characterize the potential of electrosensitization for tumor ablation.

Other groups have introduced time intervals between trains in their PEF protocols but with the aim of either allow for heat dissipation⁵¹ or to recharge the pulse generator.^{52,53} We are aware of only 1 study that investigated how intertrain intervals affect IRE efficiency.⁵⁴ Indeed, by splitting fifty-one 50- μ s pulses in 3 trains of 17 pulses each with 30-second intervals, Jiang *et al* found increased tumor destruction.⁵⁴ In reality, these authors exploit split-dose protocols without being aware of the electrosensitization phenomenon. Moreover, they did not use this term themselves.

A critical question that needs to be addressed is what physiological mechanisms are responsible for electrosensitization. One possible mechanism of electrosensitization may involve the influx of calcium (Ca^{2+}) through the nanopores. Ca^{2+} changes impact nearly every aspect of cellular life, and therefore its intracellular concentration and localization are highly regulated.⁵⁵ Split-dose treatments prolong the time intervals when the internal Ca^{2+} is elevated, and this loss of homeostasis

may cause cell death through both necrosis and apoptosis. The prolonged PEF treatment may also aggravate the adenosine triphosphate (ATP) demand to sustain membrane repair and ion pumps activated to restore ion gradients.⁵⁶ Therefore, one can speculate that a prolonged high demand for ATP combined with the ATP loss through pores could be a factor responsible for electrosensitization.

Future search for mechanisms responsible for electrosensitization should also focus on how PEF “prime” the cells making them hypersensitive to electroporation. The first train of pulses may increase the level of reactive oxygen species (ROS).^{57,58} A recent study reported that oxidative damage to the membrane increases its susceptibility to electroporation.⁵⁹ Hence, the PEF-induced ROS production may increase the cell membrane sensitivity to subsequent treatments. Electrosensitization may be explained by the PEF-induced colloid osmotic cell swelling phenomenon. Permeabilization of cells leads to water uptake and cell swelling due to the so-called colloid osmotic mechanism.¹⁵ The increase of cell diameter translates into a higher PEF-induced transmembrane potential and therefore increases electroporation.⁶⁰ Swelling takes tens of second, which may explain the time dynamic of the electrosensitization onset.

As of today, none of these mechanisms have been established as a cause of electrosensitization. We expect that a better understanding of the electrosensitization phenomenon will help to develop more effective PEF treatments.

The results of this *in vivo* study warrant further exploration of electrosensitization as a facilitating factor for tumor ablation by IRE. Contrary to other approaches used in combination with PEF, engaging electrosensitization does not require chemotherapeutic drugs or cytotoxic agents, and it can be easily integrated in existing IRE protocols. Electrosensitization may allow to reduce the pulse amplitude or to enlarge the distance between the PEF-delivering electrodes without losing the ablation efficiency. More research is needed to establish the optimal PEF conditions as well as to reveal the mechanisms underlying electrosensitization.

Acknowledgements

The authors would like to thank Dr. C. Jiang, Dr. M.A. Malik, and Mr. E. Yang for manufacturing the two-needle probe and Dr. R. Heller, Ms. C. Edelblute, Dr. S. Guo for the valuable discussion and help provided during the *in vivo* study.

Declaration of Conflicting Interests

The author(s) declared no potential conflicts of interest with respect to the research, authorship, and/or publication of this article.

Funding

The author(s) received the following financial support for the research, authorship, and/or publication of this article: This work was supported by a grant from Pulse Biosciences, Inc. (to O.N.P.) and by a 2015 AFOSR MURI grant (to AGP) on Nanoelectropulse-Induced Electromechanical Signaling and Control of Biological Systems, administered through Old Dominion University.

References

1. Knavel EM, Brace CL. Tumor ablation: common modalities and general practices. *Tech Vasc Interv Radiol*. 2013;16(4):192-200.
2. Jiang C, Davalos RV, Bischof JC. A review of basic to clinical studies of irreversible electroporation therapy. *IEEE Trans Biomed Eng*. 2015;62(1):4-20.
3. Rubinsky B. Irreversible electroporation in medicine. *Technol Cancer Res Treat*. 2007;6(4):255-260.
4. Bhonsle S, Bonakdar M, Neal RE II, et al. Characterization of irreversible electroporation ablation with a validated perfused organ model. *J Vasc Interv Radiol*. 2016;27(12):1913-1922.e2.
5. Kos B, Voigt P, Miklavcic D, Moche M. Careful treatment planning enables safe ablation of liver tumors adjacent to major blood vessels by percutaneous irreversible electroporation (IRE). *Radiol Oncol*. 2015;49(3):234-241.
6. Sano MB, Fan RE, Hwang GL, Sonn GA, Xing L. Production of spherical ablations using nonthermal irreversible electroporation: a laboratory investigation using a single electrode and grounding pad. *J Vasc Interv Radiol*. 2016;27(9):1432-1440.e3.
7. Nuccitelli R, Pliquett U, Chen X, et al. Nanosecond pulsed electric fields cause melanomas to self-destruct. *Biochem Biophys Res Commun*. 2006;343(2):351-360.
8. Nuccitelli R, Chen X, Pakhomov AG, et al. A new pulsed electric field therapy for melanoma disrupts the tumor's blood supply and causes complete remission without recurrence. *Int J Cancer*. 2009;125(2):438-445.
9. Nuccitelli R, Tran K, Sheikh S, Athos B, Kreis M, Nuccitelli P. Optimized nanosecond pulsed electric field therapy can cause murine malignant melanomas to self-destruct with a single treatment. *Int J Cancer*. 2010;127(7):1727-1736.
10. Beebe SJ, Fox PM, Rec LJ, Willis EL, Schoenbach KH. Nanosecond, high-intensity pulsed electric fields induce apoptosis in human cells. *FASEB J*. 2003;17(11):1493-1495.
11. Napotnik TB, Wu YH, Gundersen MA, Miklavcic D, Vernier PT. Nanosecond electric pulses cause mitochondrial membrane permeabilization in Jurkat cells. *Bioelectromagnetics*. 2012;33(3):257-264.
12. White JA, Blackmore PF, Schoenbach KH, Beebe SJ. Stimulation of capacitative calcium entry in HL-60 cells by nanosecond pulsed electric fields. *J Biol Chem*. 2004;279(22):22964-22972.
13. Semenov I, Xiao S, Pakhomov AG. Primary pathways of intracellular Ca(2+) mobilization by nanosecond pulsed electric field. *Biochim Biophys Acta*. 2013;1828(3):981-989.
14. Semenov I, Xiao S, Pakhomova ON, Pakhomov AG. Recruitment of the intracellular Ca2+ by ultrashort electric stimuli: the impact of pulse duration. *Cell Calcium*. 2013;54(3):145-150.
15. Nesin OM, Pakhomova ON, Xiao S, Pakhomov AG. Manipulation of cell volume and membrane pore comparison following single cell permeabilization with 60- and 600-ns electric pulses. *Biochim Biophys Acta*. 2011;1808(3):792-801.
16. Craviso GL, Choe S, Chatterjee I, Vernier PT. Modulation of intracellular Ca2+ levels in chromaffin cells by nanoelectropulses. *Bioelectrochemistry*. 2012;87:244-252.

17. Vernier PT, Sun Y, Marcu L, Salemi S, Craft CM, Gundersen MA. Calcium bursts induced by nanosecond electric pulses. *Biochem Biophys Res Commun.* 2003;310(2):286-295.
18. Berghofer T, Eing C, Flickinger B, et al. Nanosecond electric pulses trigger actin responses in plant cells. *Biochem Biophys Res Commun.* 2009;387(3):590-595.
19. Rassokhin MA, Pakhomov AG. Electric field exposure triggers and guides formation of pseudopod-like blebs in U937 monocytes. *J Membr Biol.* 2012;245(9):521-529.
20. Pakhomov AG, Xiao S, Pakhomova ON, Semenov I, Kuipers MA, Ibey BL. Disassembly of actin structures by nanosecond pulsed electric field is a downstream effect of cell swelling. *Bioelectrochemistry.* 2014;100:88-95.
21. Thompson GL, Roth C, Tolstykh G, Kuipers M, Ibey BL. Disruption of the actin cortex contributes to susceptibility of mammalian cells to nanosecond pulsed electric fields. *Bioelectromagnetics.* 2014;35(4):262-272.
22. Morotomi-Yano K, Akiyama H, Yano K. Nanosecond pulsed electric fields activate AMP-activated protein kinase: implications for calcium-mediated activation of cellular signaling. *Biochem Biophys Res Commun.* 2012;428(3):371-375.
23. Morotomi-Yano K, Akiyama H, Yano K. Nanosecond pulsed electric fields induce poly(ADP-ribose) formation and non-apoptotic cell death in HeLa S3 cells. *Biochem Biophys Res Commun.* 2013;438(3):557-562.
24. Tolstykh GP, Beier HT, Roth CC, Thompson GL, Ibey BL. 600 ns pulse electric field-induced phosphatidylinositol4,5-bisphosphate depletion. *Bioelectrochemistry.* 2014;100:80-87.
25. Ibey BL, Pakhomov AG, Gregory BW, et al. Selective cytotoxicity of intense nanosecond-duration electric pulses in mammalian cells. *Biochim Biophys Acta.* 2010;1800(11):1210-1219.
26. Pakhomova ON, Gregory BW, Semenov I, Pakhomov AG. Two modes of cell death caused by exposure to nanosecond pulsed electric field. *PLoS One.* 2013;8(7): e70278.
27. Ren W, Beebe SJ. An apoptosis targeted stimulus with nanosecond pulsed electric fields (nsPEFs) in E4 squamous cell carcinoma. *Apoptosis.* 2011;16(4):382-393.
28. Pakhomova ON, Gregory BW, Khorokhorina VA, Bowman AM, Xiao S, Pakhomov AG. Electroporation-induced electrosensitization. *PLoS One.* 2011;6(2):e17100.
29. Vernier PT, Sun Y, Gundersen MA. Nanoelectropulse-driven membrane perturbation and small molecule permeabilization. *BMC Cell Biol.* 2006;7:37.
30. Silve A, Guimera Brunet A, Al-Sakere B, Ivorra A, Mir LM. Comparison of the effects of the repetition rate between microsecond and nanosecond pulses: electroporation-induced electro-desensitization? *Biochim Biophys Acta.* 2014;1840(7): 2139-2151.
31. Lamberti P, Romeo S, Sannino A, Zeni L, Zeni O. The role of pulse repetition rate in nsPEF-induced electroporation: a biological and numerical investigation. *IEEE Trans Biomed Eng.* 2015; 62(9):2234-2243.
32. Sano MB, Arena CB, Bittleman KR, et al. Bursts of bipolar microsecond pulses inhibit tumor growth. *Sci Rep.* 2015;5:14999.
33. Sweeney DC, Rebersek M, Dermol J, Rems L, Miklavcic D, Davalos RV. Quantification of cell membrane permeability induced by monopolar and high-frequency bipolar bursts of electrical pulses. *Biochim Biophys Acta.* 2016;1858(11):2689-2698.
34. Muratori C, Casciola M, Pakhomova O. Electric pulse repetition rate: sensitization and desensitization. In: Miklavcic D, ed. *Handbook of Electroporation.* Boca Raton, FL: Springer International Publishing AG; 2016:1-16.
35. Pakhomova ON, Gregory BW, Pakhomov AG. Facilitation of electroporative drug uptake and cell killing by electrosensitization. *J Cell Mol Med.* 2013;17(1):154-159.
36. Dermol J, Pakhomova ON, Pakhomov AG, Miklavcic D. Cell electrosensitization exists only in certain electroporation buffers. *PLoS One.* 2016;11(7):e0159434.
37. Muratori C, Pakhomov AG, Xiao S, Pakhomova ON. Electrosensitization assists cell ablation by nanosecond pulsed electric field in 3D cultures. *Sci Rep.* 2016;6:23225.
38. Breton M, Mir LM. Microsecond and nanosecond electric pulses in cancer treatments. *Bioelectromagnetics.* 2012;33(2):106-123.
39. Linnert M, Gehl J. Bleomycin treatment of brain tumors: an evaluation. *Anticancer Drugs.* 2009;20(3):157-164.
40. Sersa G, Miklavcic D, Cemazar M, Rudolf Z, Pucihar G, Snoj M. Electrochemotherapy in treatment of tumours. *Eur J Surg Oncol.* 2008;34(2):232-240.
41. Kaneko T, LePage GA, Shnitka TK. KLN205—a murine lung carcinoma cell line. *In Vitro.* 1980;16(10):884-892.
42. Dermol J, Pakhomova ON, Xiao S, Pakhomov AG, Miklavcic D. Cell sensitization is induced by a wide range of permeabilizing electric fields. In: Jarm T, Kramar P, eds. *1st World Congress on Electroporation and Pulsed Electric Fields in Biology, Medicine and Food & Environmental Technologies.* Vol 53. Singapore: Springer; 2016:163-166.
43. Pakhomov AG, Semenov I, Casciola M, Xiao S. Neuronal excitation and permeabilization by 200-ns pulsed electric field: an optical membrane potential study with FluoVolt dye. *Biochim Biophys Acta.* 2017;1859(7):1273-1281.
44. Ibey BL, Xiao S, Schoenbach KH, Murphy MR, Pakhomov AG. Plasma membrane permeabilization by 60- and 600-ns electric pulses is determined by the absorbed dose. *Bioelectromagnetics.* 2009;30(2):92-99.
45. Merla C, Denzi A, Paffi A, et al. Novel passive element circuits for microdosimetry of nanosecond pulsed electric fields. *IEEE Trans Biomed Eng.* 2012;59(8):2302-2311.
46. Pakhomov AG, Gianulis E, Vernier PT, Semenov I, Xiao S, Pakhomova ON. Multiple nanosecond electric pulses increase the number but not the size of long-lived nanopores in the cell membrane. *Biochim Biophys Acta.* 2015;1848(4):958-966.
47. Pakhomov AG, Bowman AM, Ibey BL, Andre FM, Pakhomova ON, Schoenbach KH. Lipid nanopores can form a stable, ion channel-like conduction pathway in cell membrane. *Biochem Biophys Res Commun.* 2009;385(2):181-186.
48. Schwartz M. A biomathematical approach to clinical tumor growth. *Cancer.* 1961;14:1272-1294.
49. Neal RE II, Davalos RV. The feasibility of irreversible electroporation for the treatment of breast cancer and other heterogeneous systems. *Ann Biomed Eng.* 2009;37(12):2615-2625.
50. Arena CB, Szot CS, Garcia PA, Rylander MN, Davalos RV. A three-dimensional in vitro tumor platform for modeling

- therapeutic irreversible electroporation. *Biophys J.* 2012;103(9):2033-2042.
51. Al-Sakere B, Andre F, Bernat C, et al. Tumor ablation with irreversible electroporation. *PLoS One.* 2007;2(11):e1135.
52. Deodhar A, Monette S, Single GW Jr, et al. Renal tissue ablation with irreversible electroporation: preliminary results in a porcine model. *Urology.* 2011;77(3):754-760.
53. Garcia PA, Rossmeisl JH Jr, Neal RE II, et al. Intracranial non-thermal irreversible electroporation: in vivo analysis. *J Membr Biol.* 2010;236(1):127-136.
54. Jiang C, Shao Q, Bischof J. Pulse timing during irreversible electroporation achieves enhanced destruction in a hindlimb model of cancer. *Ann Biomed Eng.* 2015;43(4):887-895.
55. Berridge MJ, Bootman MD, Roderick HL. Calcium signalling: dynamics, homeostasis and remodelling. *Nat Rev Mol Cell Biol.* 2003;4(7):517-529.
56. Idone V, Tam C, Andrews NW. Two-way traffic on the road to plasma membrane repair. *Trends Cell Biol.* 2008;18(11):552-559.
57. Bonnafous P, Vernhes M, Teissie J, Gabriel B. The generation of reactive-oxygen species associated with long-lasting pulse-induced electroporabilisation of mammalian cells is based on a non-destructive alteration of the plasma membrane. *Biochim Biophys Acta.* 1999;1461(1):123-134.
58. Pakhomova ON, Khorokhorina VA, Bowman AM, et al. Oxidative effects of nanosecond pulsed electric field exposure in cells and cell-free media. *Arch Biochem Biophys.* 2012;527(1):55-64.
59. Vernier PT, Levine ZA, Wu YH, et al. Electroporating fields target oxidatively damaged areas in the cell membrane. *PLoS One.* 2009;4(11):e7966.
60. Grosse C, Schwan HP. Cellular membrane potentials induced by alternating fields. *Biophys J.* 1992;63(6):1632-1642.